

## P-3-12

## An Analysis of Layout and Temperature Effects on Magnetic-Coupling Factor, Resistive-Coupling Factor, and Power Gain Performances of RF Transformers for RFIC Applications

Yo-Sheng Lin, Chi-Chen Chen, Yan-Ru Tzeng, and Hsiao-Bin Liang

Department of Electrical Engineering, National Chi-Nan University, Puli, Taiwan, R.O.C.

Phone: 886-4-92912198, Fax: 886-4-92917810, Email : stephenlin@ncnu.edu.tw

**Abstract** - In this paper, we demonstrate a comprehensive analysis of the temperature effect ( $-25^{\circ}\text{C} \sim 175^{\circ}\text{C}$ ) on the quality-factors ( $Q_1$  and  $Q_2$ ), magnetic-coupling factor ( $K_{\text{Im}}$ ), resistive-coupling factor ( $K_{\text{Re}}$ ), maximum available power gain ( $G_{\text{Amax}}$ ), and minimum noise figure ( $\text{NF}_{\text{min}}$ ) performances of RF bifilar and stacked transformers for RFIC applications. Excellent  $G_{\text{Amax}}$  of 0.713 and 0.806 (i.e.  $\text{NF}_{\text{min}}$  of 1.469 dB and 0.937 dB) were achieved at 5 GHz and 7 GHz, respectively, at room temperature (RT), for a 1:1 stacked transformer mainly due to its high  $K_{\text{Im}}$  and  $K_{\text{Re}}$ . In addition, for the 1:1 bifilar transformer at RT, though its  $K_{\text{Im}}$  and  $K_{\text{Re}}$  are low, good  $G_{\text{Amax}}$  of 0.636 and 0.631 (i.e.  $\text{NF}_{\text{min}}$  of 1.965 dB and 2.0 dB) were still achieved at 5 GHz and 7 GHz, respectively, mainly due to its high  $Q_1$  and  $Q_2$ .

### I. Introduction

In the design of ultra-low-voltage high-performance transformer-feedback VCOs [1] and LNAs [2], the power gain  $G_A$  (or noise figure NF) performance of the transformers used are crucial for the phase noise performance of the VCOs and the NF performance of the LNAs. However, the  $G_A$  (or NF) performance of monolithic RF transformers fabricated on normal silicon substrates are not satisfactory up to now mainly due to the  $K_{\text{Im}}$ , the  $K_{\text{Re}}$ , and the quality-factors (of the primary and the secondary coil) which are not high enough [3]. Various methods have been proposed to improve the Q-factors of RF passive devices, such as high-resistivity silicon, front-side and backside micromachining, porous silicon, proton implantation, and substrate transfer [3]. However, no detailed analyses of the layout and the temperature effects on the  $K_{\text{Im}}$  and  $K_{\text{Re}}$  performances of various important RF transformers have been reported. Therefore, in this work, we demonstrate an analysis of the temperature effect ( $-25^{\circ}\text{C} \sim 175^{\circ}\text{C}$ ) on the quality-factors ( $Q_1$  and  $Q_2$ ),  $K_{\text{Im}}$ ,  $K_{\text{Re}}$ ,  $G_{\text{Amax}}$ , and  $\text{NF}_{\text{min}}$  performances of RF bifilar and stacked transformers for RFIC applications.

### II. Transformer Structure

The transformers under study were fabricated with a  $0.18\text{ }\mu\text{m}$  RF CMOS technology on a p-type silicon substrate (resistivity :  $10\text{ }\Omega\text{-cm}$ ) with thickness of  $700\text{ }\mu\text{m}$ . The main features of the backend processes are as follows. There are 6 metal layers, named M1 to M6 from the bottom to the top. The thickness of M6 is  $0.99\text{ }\mu\text{m}$ , and that of M1-M5 is  $0.53\text{ }\mu\text{m}$ . Fig. 1 shows the 3D schematic diagrams of the 1:1 bifilar transformer (transformer-A), and the 1:1 stacked transformer (transformer-B). Table I is a summary of the primary layout parameters and the extracted small-signal equivalent circuit parameters of transformers A-E.

### III. Measurement Results and Discussions

The frequency-dependent S-parameter measurements were performed from 0.1 GHz to 20 GHz by an HP-8510C

network analyzer. Fig. 2(a) shows the measured equivalent Q-factors of the primary coil ( $Q_1$ ) and the secondary coil ( $Q_2$ ) of transformer-A and transformer-B. Good  $Q_1$  of 8.8 and 9.4,  $Q_2$  of 7.5 and 7.1 were achieved at 5 GHz and 7 GHz, respectively, for transformer-A. This is better than that (i.e.  $Q_1$  of 5.8 and 1.6,  $Q_2$  of 3.6 and 1.6 at 5 GHz and 7 GHz, respectively) of the transformer-B. The higher  $Q_1$  and  $Q_2$ , and the larger self-resonance frequency of the primary coil ( $f_{\text{SR1}}$ ) and the secondary coil ( $f_{\text{SR2}}$ ) of transformer-A are attributed to its lower series metal resistances  $R_{s1}$  and  $R_{s2}$ , and lower parasitic (or overlap) capacitance  $C_p$  between the primary coil and the secondary coil (see Table I). Fig. 2(b) shows the measured  $K_{\text{Im}}$  and  $K_{\text{Re}}$  of transformer-A and transformer-B. As can be seen, high  $K_{\text{Im}}$  of 1.083 and 1.009,  $K_{\text{Re}}$  of 0.487 and 0.977 were achieved at 5 GHz and 7 GHz, respectively, for transformer-B. This is better than that (i.e.  $K_{\text{Im}}$  of 0.536 and 0.522,  $K_{\text{Re}}$  of 0.111 and 0.15 at 5 GHz and 7 GHz, respectively) of transformer-A. The higher  $K_{\text{Im}}$  and  $K_{\text{Re}}$  of transformer-B is attributed to its smaller equivalent vertical distance (VD) [4].

Fig. 3(a) shows the measured  $Q_1$  and  $Q_2$  of transformer-A at various temperatures. As can be seen, the measured  $Q_1$  and  $Q_2$  decrease with the increase of temperature mainly due to the positive temperature coefficient of the series metal resistance  $R_{s1}$  and  $R_{s2}$ . The measured temperature dependence of  $R_{1\text{-eff}}$  at low frequencies (i.e.  $R_{s1}$ ) is linear. The corresponding temperature coefficient is  $3.94 \times 10^{-3}/^{\circ}\text{C}$  at 0.1 GHz, which is very close to the result ( $3.9 \times 10^{-3}/^{\circ}\text{C}$ ) reported in the literature. Fig. 3(b) shows the measured  $K_{\text{Im}}$  and  $K_{\text{Re}}$  of transformer-A at various temperatures. As can be seen, the temperature dependences of both  $K_{\text{Im}}$  and  $K_{\text{Re}}$  are very weak. Fig. 6(c) shows the measured  $G_{\text{Amax}}$  both before and after the test pads were de-embedded of transformer-A at various temperatures. Fig. 7(a) shows the measured  $Q_1$  and  $Q_2$  of transformer-B at various temperatures. Fig. 7(b) shows the measured  $K_{\text{Im}}$  and  $K_{\text{Re}}$  of transformer-B at various temperatures. Fig. 7(c) shows the measured  $G_{\text{Amax}}$  of transformer-B at various temperatures both before and after the test pads were de-embedded. The same trends as those of transformer-A were observed.

### IV. Conclusions

The present analysis is helpful for RF engineers to design temperature-insensitive ultra-low-voltage high-performance transformer-feedback RF-ICs.

### Reference

- [1] K. Kwok, and H. C. Luong, *IEEE Journal of Solid-State Circuits*, vol. 40, no. 3, pp. 652-660, Mar. 2005.
- [2] D. J. Cassan, and J. R. Long, *IEEE Journal of Solid-State Circuits*, vol. 38, pp. 427-435, Mar. 2003.
- [3] K. T. Ng, B. Rejaei, and J. N. Burghartz, *IEEE Trans. on Microwave Theory and Techniques* vol. 50, no. 1, pp. 377-383, Jan. 2002.
- [4] H. M. Hsu, *IEEE Trans. on Electron Devices*, vol. 52, no. 7, pp. 1410-1414, Jul. 2005.

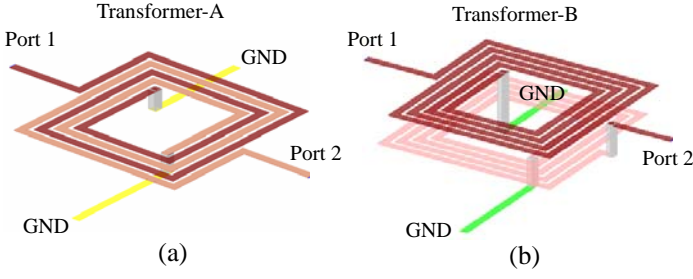


Fig. 1 The 3D schematic diagrams of (a) transformer-A, and (b) transformer-B.

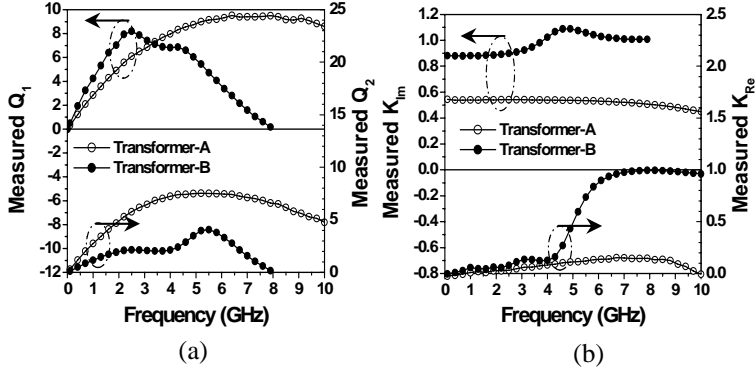


Fig. 2 The measured (a)  $Q_1$  and  $Q_2$ , and (b)  $K_{IM}$  and  $K_{Re}$  of transformers A-B.

Table I Summary of the primary layout parameters and the extracted SSC parameters of transformers A-E.

Technology	0.18 $\mu\text{m}$ 1P6M CMOS Process (substrate resistivity: 10 $\Omega\cdot\text{cm}$ , substrate thickness : 750 $\mu\text{m}$ )				
Transformer ID	A	B	C	D	E
Structure	Bifilar	Stacked (STD)	Stacked (offset)	Stacked (offset)	Stacked (offset)
W ( $\mu\text{m}$ )	10				
S ( $\mu\text{m}$ )	5	5	10	10	10
Turn number (N)	2	4	4	4	4
Turn Ratio	1:1	1:1	1:2	1:3	1:4
Primary Coil	M6	M6	M5	M5	M4
Secondary Coil	M6	M5	M6 & M4	M6 & M4-M3	M6-M5 & M3-M2
Overall Dimension ( $\mu\text{m}\times\mu\text{m}$ )	240 $\times$ 240				
Inner Dimension ( $\mu\text{m}\times\mu\text{m}$ )	100 $\times$ 130		60 $\times$ 70		60 $\times$ 60
Range (GHz)	0.1 - 10	0.1 - 8	0.1 - 3	0.1 - 1.45	0.1 - 1.425
$R_{s1}$ ( $\Omega$ )	3.9	7.26	23.37	23.69	24.38
$L_{s1}$ (nH)	1.89	5.86	4.08	4.15	4.10
$R_{s2}$ ( $\Omega$ )	4.1	27.12	25.53	48.35	69.20
$L_{s2}$ (nH)	1.94	5.58	13.51	28.53	49.70
M (nH)	1.03	4.78	6.39	9.80	12.82
K	0.58	0.89	0.861	0.900	0.898
$C_p$ (fF)	62.7	633.4	204	358.2	394.6
$C_{ox1}$ (fF)	54.3	167.4	121.4	148.2	146.6
$C_{ox2}$ (fF)	57.3	186.1	436	691.6	761.4
$C_{sub1}$ (fF)	4.3	30.0	125.9	145.8	162.8
$R_{sub1}$ ( $\Omega$ )	2277.2	3167.7	206.6	768.6	851
$C_{sub2}$ (fF)	10.9	50.4	417.3	376.4	269
$R_{sub2}$ ( $\Omega$ )	1660.2	3248.1	1444.4	1520.8	2027.7

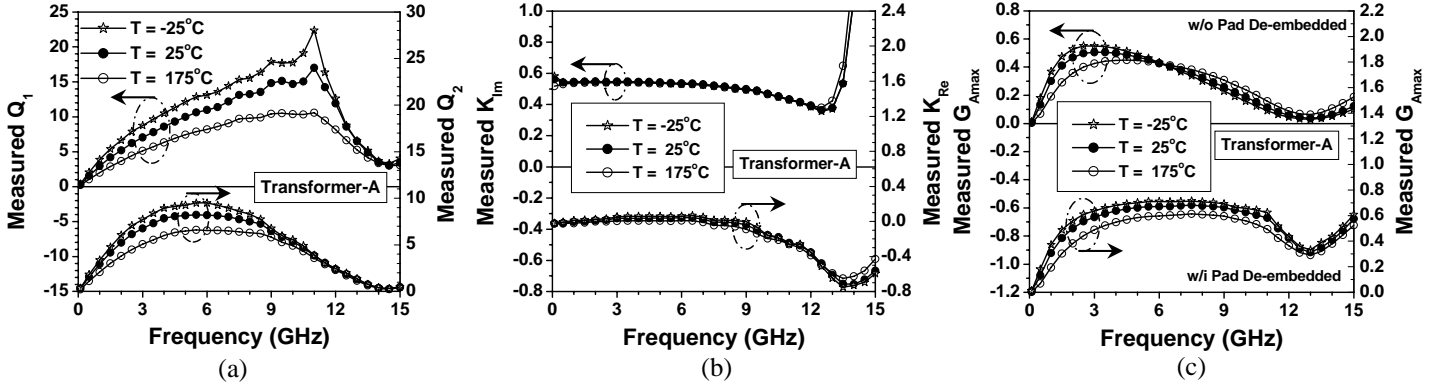


Fig. 3 The measured (a)  $Q_1$  and  $Q_2$ , (b)  $K_{IM}$  and  $K_{Re}$ , and (c)  $G_{Amix}$  (both before and after the test pads were de-embedded) of transformer-A at various temperatures ( $-25^\circ\text{C}$ ,  $25^\circ\text{C}$ , and  $175^\circ\text{C}$ ).

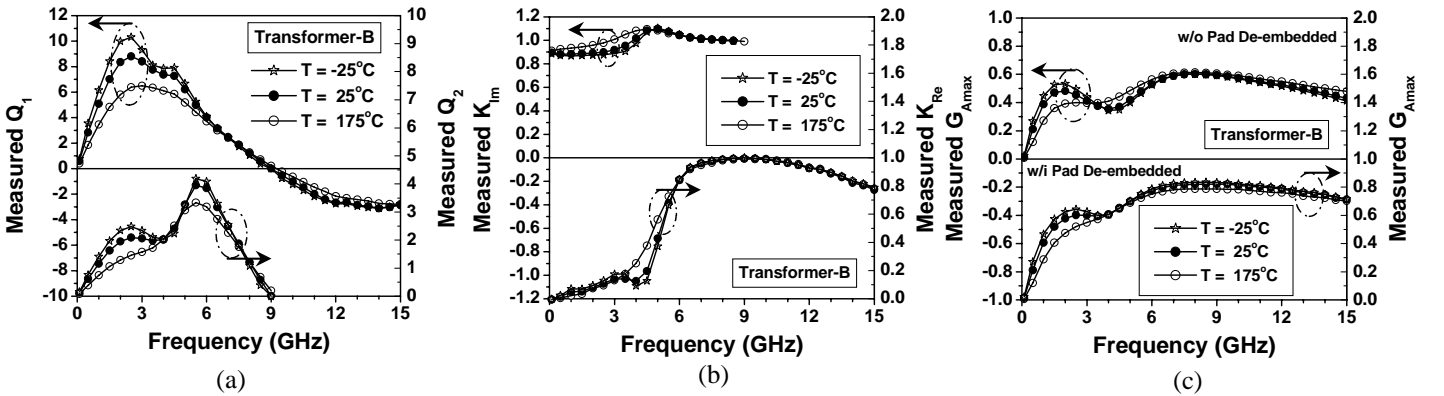


Fig. 4 The measured (a)  $Q_1$  and  $Q_2$ , (b)  $K_{IM}$  and  $K_{Re}$ , and (c)  $G_{Amix}$  (both before and after the test pads were de-embedded) of transformer-B at various temperatures ( $-25^\circ\text{C}$ ,  $25^\circ\text{C}$ , and  $175^\circ\text{C}$ ).